

Background

There is a growing need for novel agents to treat resistant GIST. The goal of this study was to characterize and identify potential therapeutic targets in the metabolic profile of GIST.

Methods

Human GIST T1 cells were incubated with imatinib 0.5 μ M with harvesting at time 0, 24 hrs and 48 hrs. Tumor, adjacent control tissue samples from 10 patients (Seven exposed to imatinib or sunitinib) and three tumor samples from xenografts in nude mice models (no TKI exposure) were extracted for analysis. ¹H-NMR spectra, using a 500MHz spectrometer equipped with a cryoprobe head, were acquired and processed. Energy state, glucose (cytosolic glycolysis versus mitochondrial Krebs cycle), protein and lipid metabolism (indicators of proliferation and invasiveness) metabolomic profiles were assessed globally in correlation with clinical and histopathologic findings.

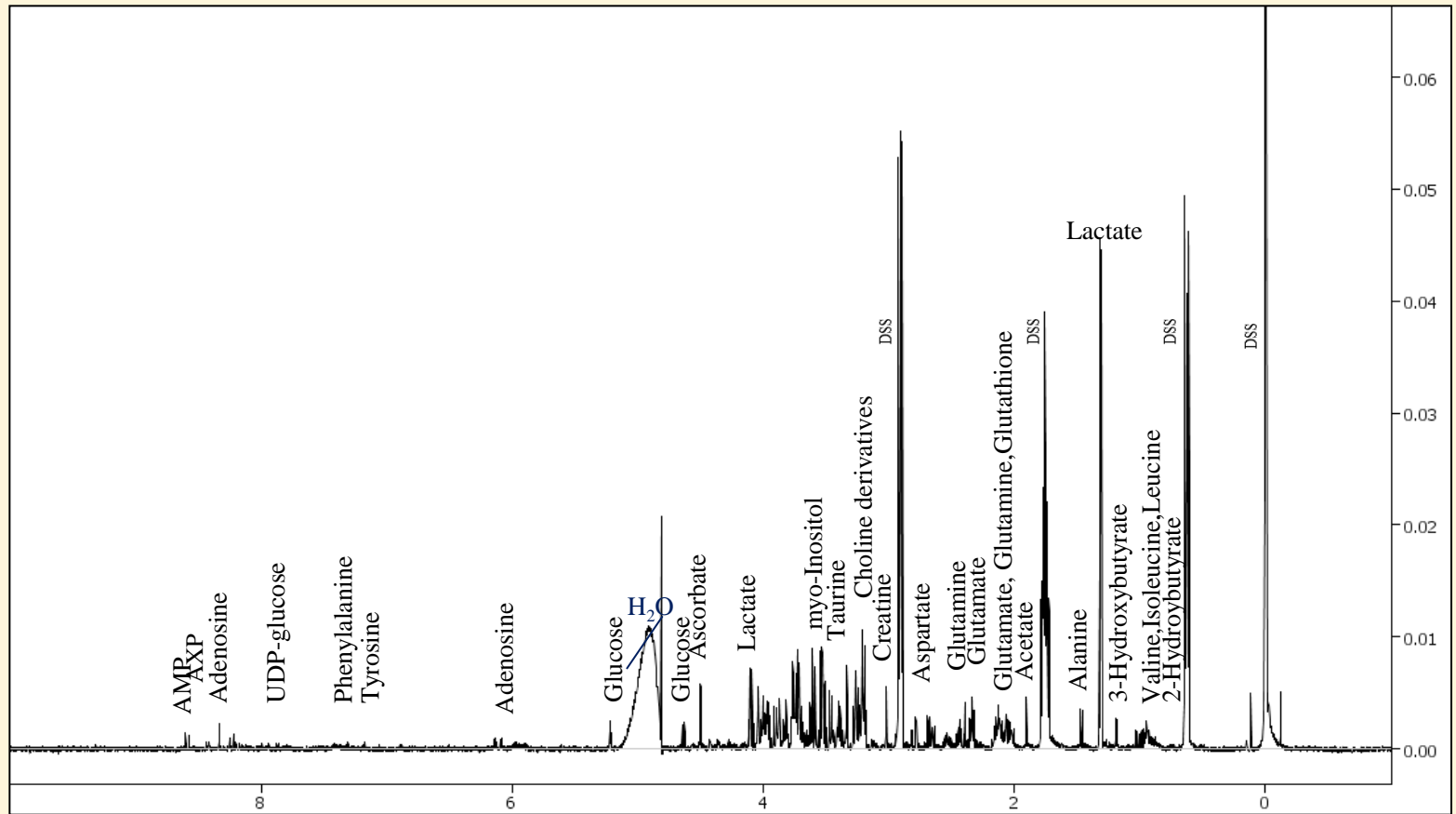


Figure 1. GIST tissue NMR spectrum with some of the metabolite assignments

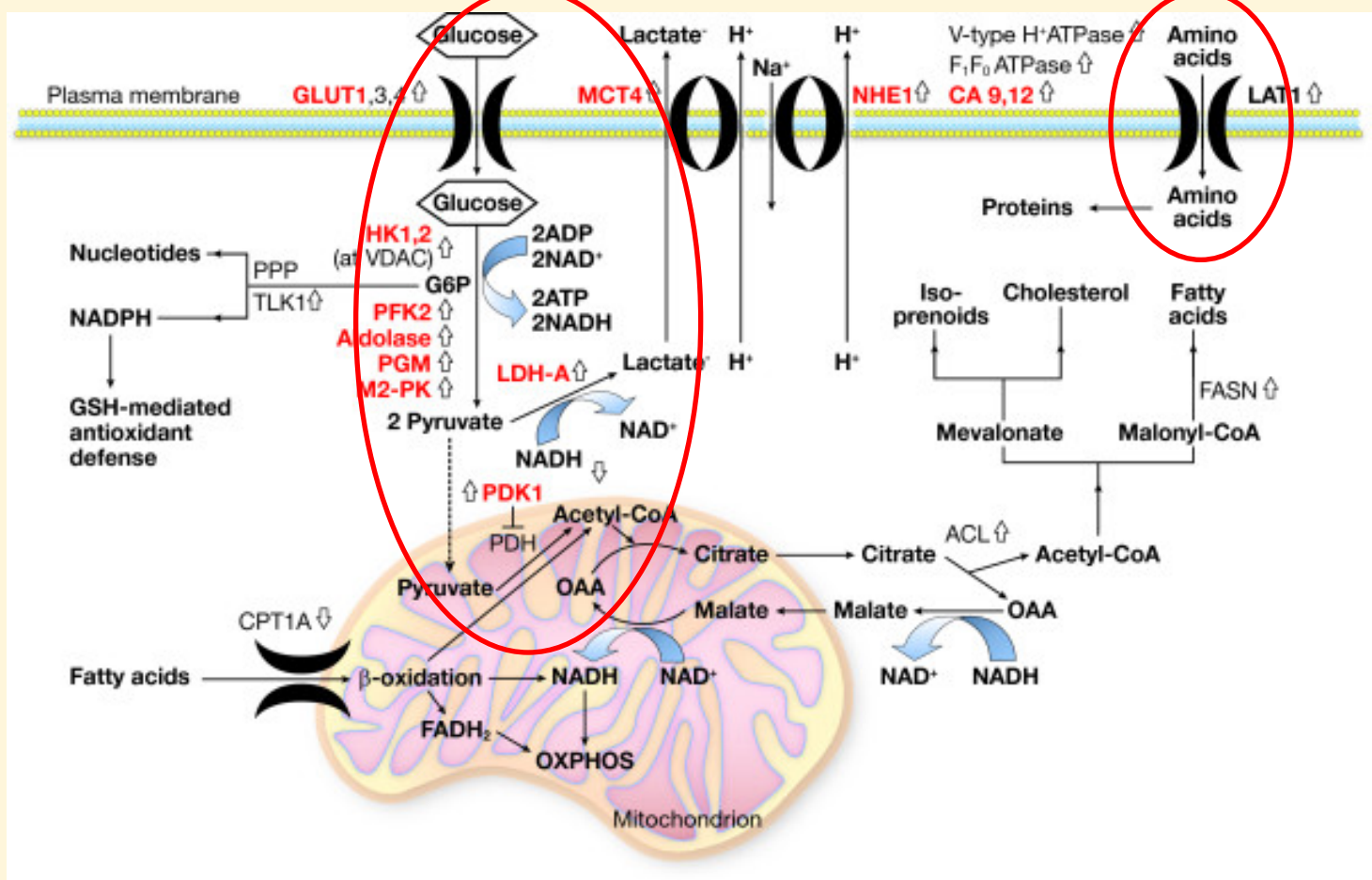


Figure 4. Schematic diagram of altered metabolic pathways in cancer cells

Table 1. Clinical characteristics of involved patients

Sample ID	Age	Sex	Race	Site	Treatment at time of sampling	Clinical response	GIST subtype	Size in cms	% viable	Mitoses /50 HPF	Exon 9	Exon 11	PDGFRA
T1	68	M	Hispanic	stomach	Imatinib	Minimal	spindle	2.6	100	>10	0	0	0
T2	57	M	Caucasian	stomach	Imatinib	Marked	spindle	13	50	0	0	1	1
T3	64	F	Caucasian	sigmoid colon	Sunitinib	Moderate	epithelioid	3	90	1	0	1	0
T4	62	F	Caucasian	stomach	Imatinib	Marked	spindle	6	5	1	0	1	0
T5	73	F	Caucasian	stomach	None	N/A	mixed	4	100	3	0	1	0
T6	67	M	Caucasian	rectum	Sunitinib	Minimal	spindle	5.5	20	0	1	0	0
T7	61	M	African Am	stomach	None	N/A	spindle	16	60	0	0	0	0
T8	42	M	Hispanic	stomach	None	N/A	spindle and epith	15	50	0	0	0	0
T9	70	M	African Am	abd wall	Imatinib	Progression	epithelioid	27	80	0	0	1	0
T10	65	F	African Am	stomach	Sunitinib	Progression	epithelioid	6	60	32	0	1	0

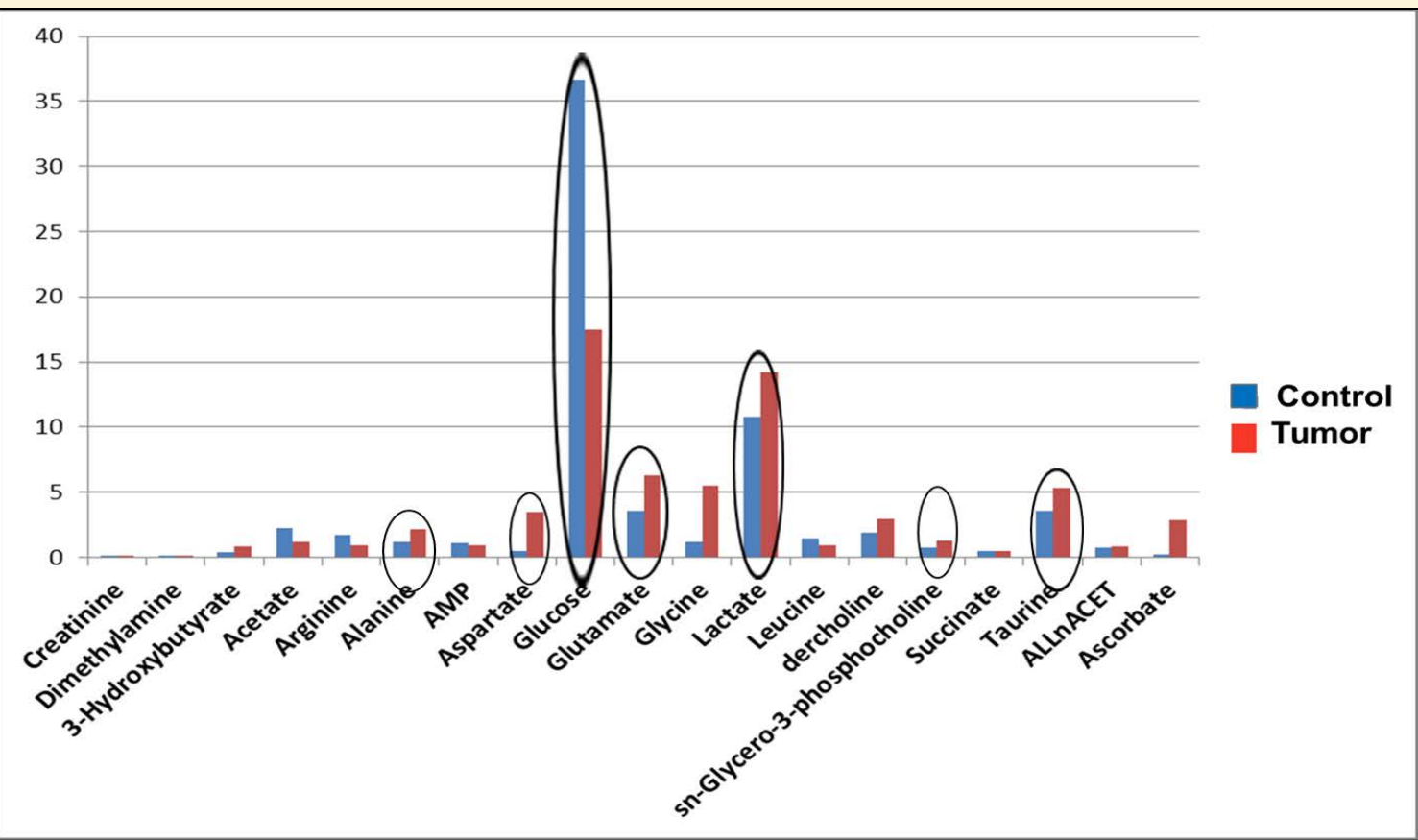


Figure 2. Metabolite concentration differences between human GIST tissue samples and normal controls

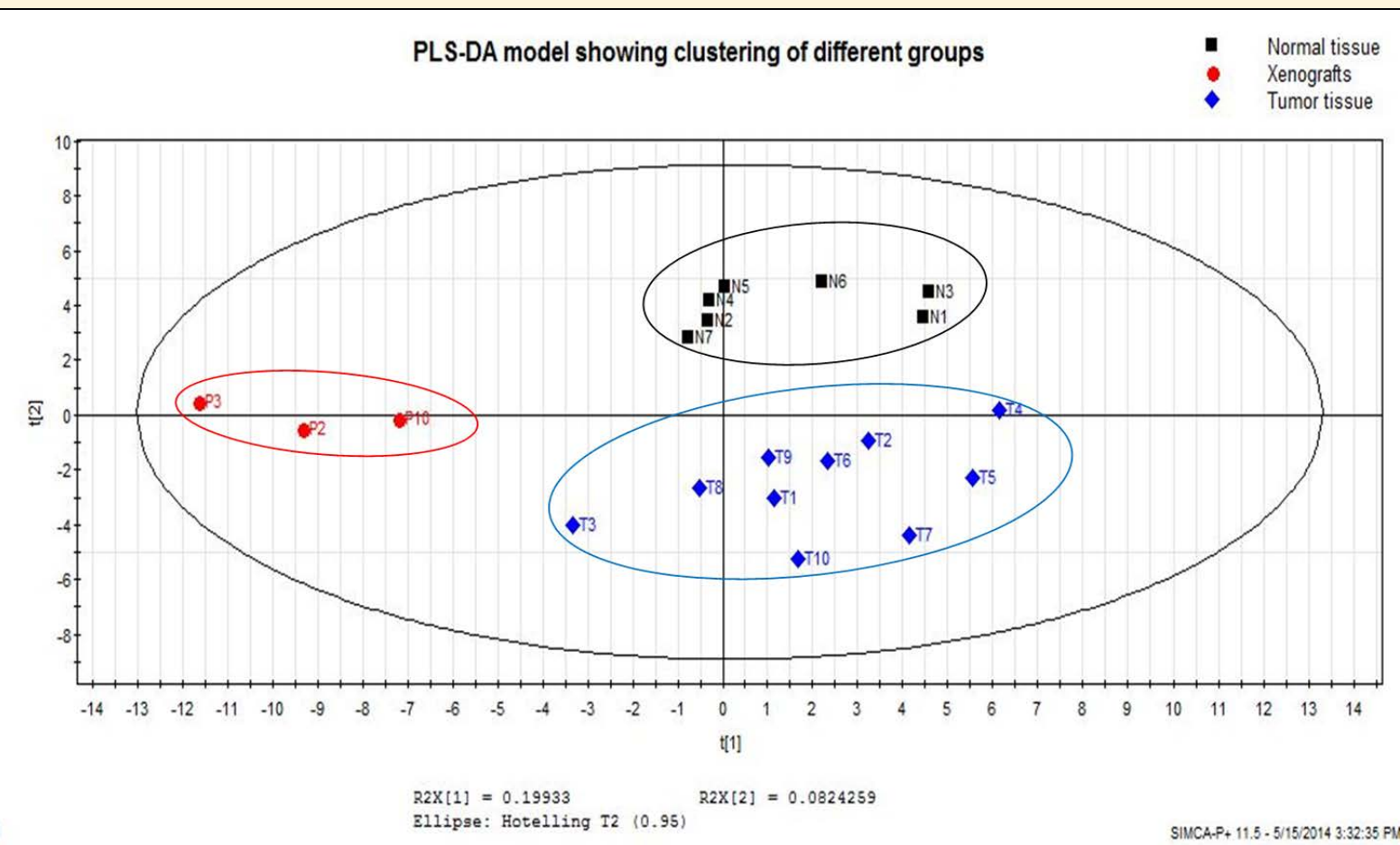


Figure 5. PLS-DA model showing clustering of tumor tissues (T), from normal controls (N), from xenografts (P) (R²Y=0.56).

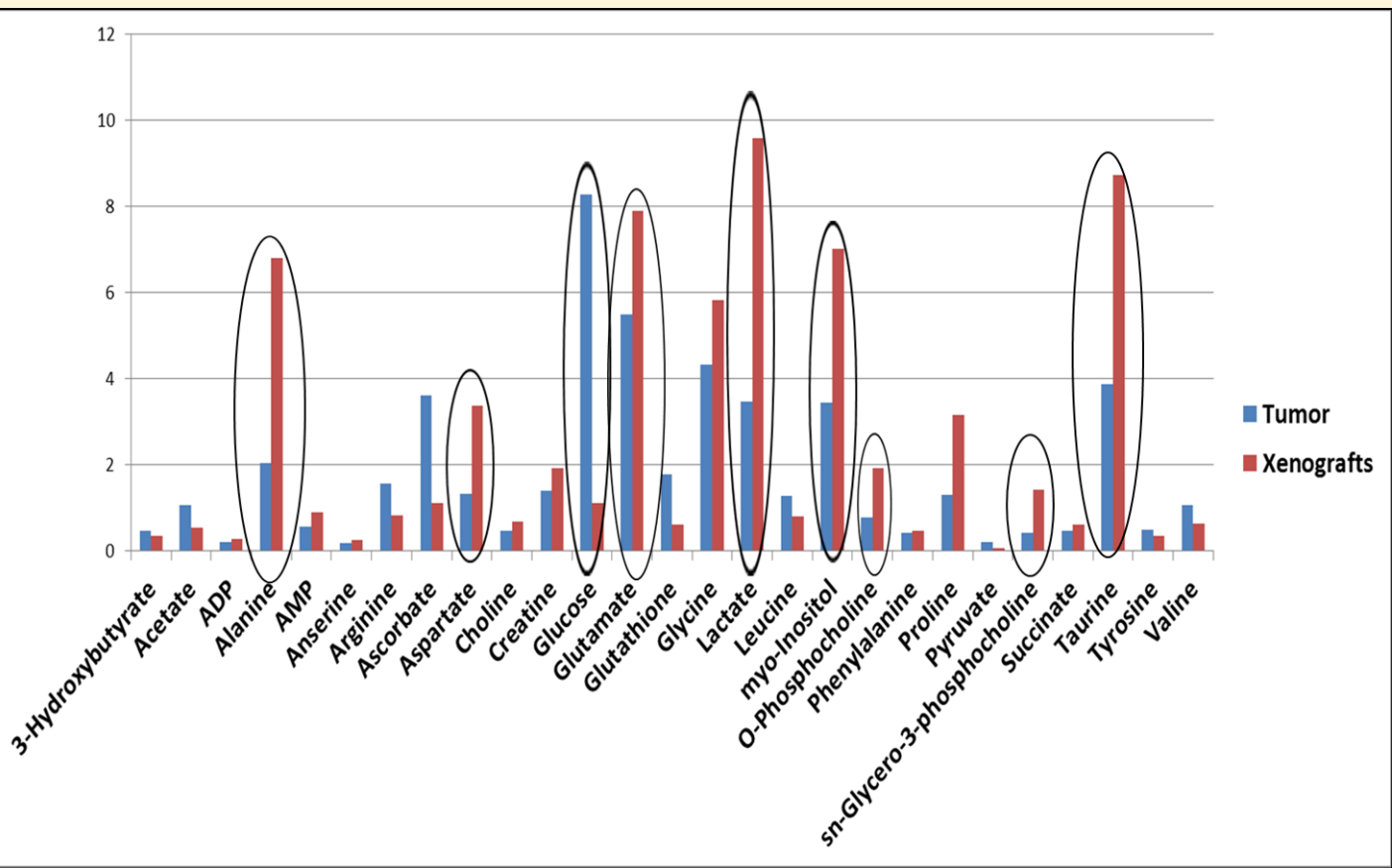


Figure 3. Metabolite concentration differences between human GIST tissue samples and Xenografts

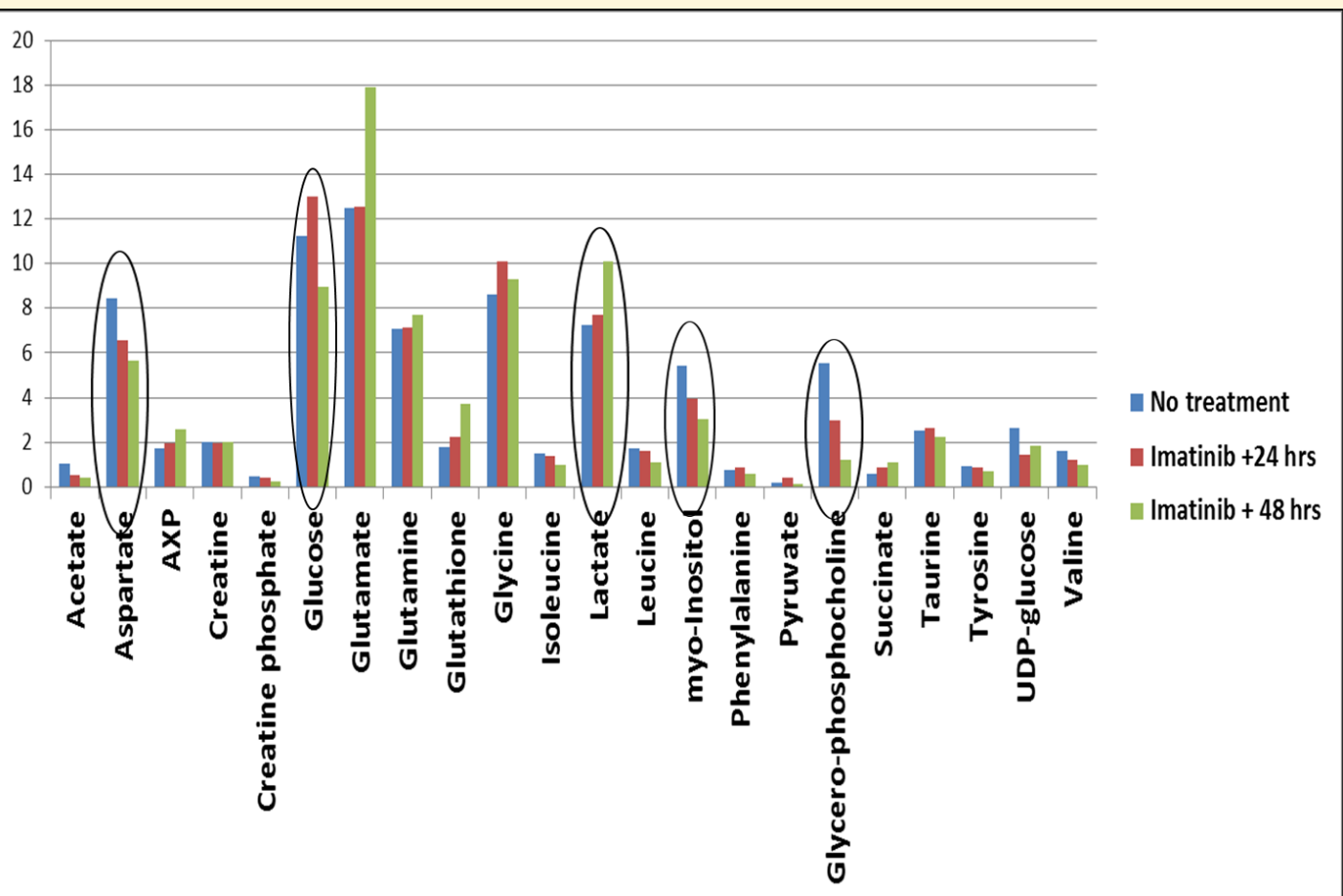


Figure 6. GIST cell line extracts metabolite concentration trends over time when incubated with imatinib mesylate (spectra referenced to DSS, normalized data)

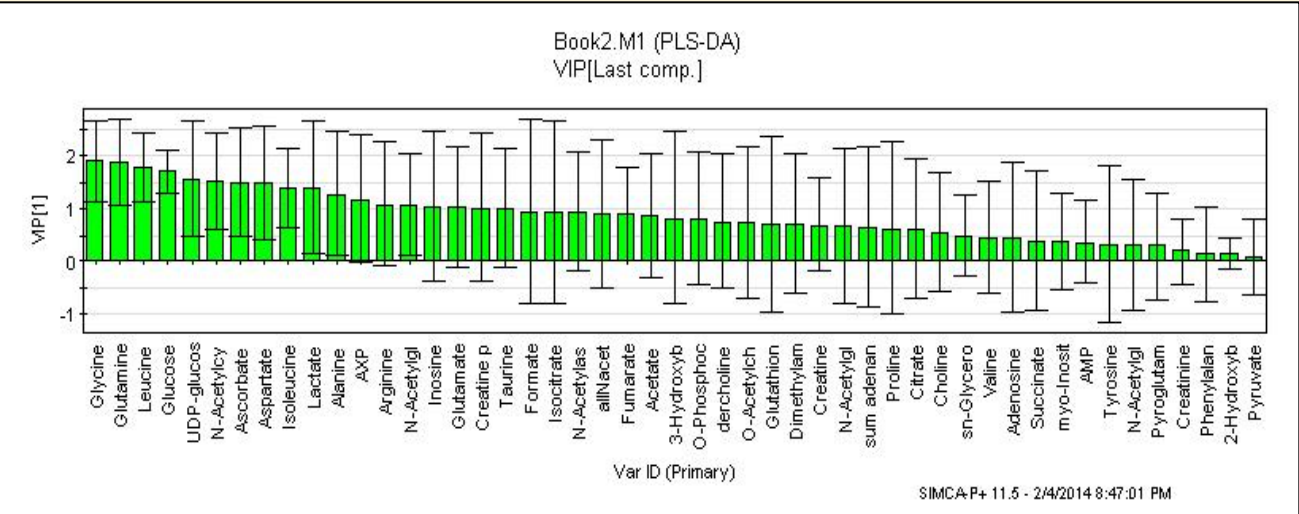


Figure 7. Variable importance in cluster separation of tissue samples.

Results

Findings in cell lines, tissues and xenografts suggest shift from cytosolic glycolysis (glucose decrease and increased lactate with minimal changes in pyruvate) towards the mitochondrial Krebs cycle (elevated glutamine and glutamate synthesis) in all tumor samples. Aspartate, myoinositol, and cell membrane phospholipids such as phosphocholine/ glycerophosphocholine were greater in untreated GIST xenografts compared to treated tumors. Alanine, taurine, proline, ADP and phosphocholine were significantly higher in tumor tissue extracts compared to control (imatinib treated) (p<0.05). Tumor stage, mitotic index or mutation type did not correlate with metabolomics profile. Differences were accentuated among untreated patients. Partial Least Squares-Discriminant Analysis (PLS-DA) model successfully separated tumor tissues from controls (R²Y=0.56).

Conclusion

Metabolomic profiling of GIST cell lines, patient and xenograft GIST samples exposed to KIT inhibitors suggest that cytosolic glycolysis and phospholipid biology may be important not only in the GIST phenotype but may be ameliorated with KIT inhibition by imatinib. Further understanding of GIST metabolomics may lead to the identification of new therapeutic targets.